Capillary length of a planar interface from low temperatures to the critical point: An Ising $d=2$ strip

J. Stecki
Institute of Physical Chemistry of the Polish Academy of Sciences, ulica Kasprzaka 44/52, 01-224 Warszawa 42, Poland
(Received 11 August 1992)

The correlation length controlling the long-range decay of the density-density correlation function in the direction parallel to the interface is computed exactly, for $T \leq T_c$, in the two-dimensional Ising $M \times \infty$ strip periodic in the long direction with a $(+/-)$ boundary condition in the other direction which creates a planar strongly fluctuating interface. A crossover from long-range capillary-wave-like behavior to short-range bulk correlations above T_c, a new scaling function, and corrections to scaling at T_c are found.

I. INTRODUCTION

Fluctuations of the planar interface between two coexisting phases are described at low temperatures by capillary-wave theory.[1] The latter correctly predicts long-range correlations in the direction along the interface.[2] The decay is exponential and the relevant correlation length is known.

It is a matter of conjecture as to what happens to this correlation length if we raise the temperature and approach the critical point. The capillary-wave theory deals with two incompressible bulk phases separated by an instantaneous mathematical surface; the bulk density fluctuations in either phase are neglected entirely. There is no recipe for incorporating the density fluctuations into the capillary-wave picture. Clearly a quantitative description of the crossover from the low-temperature capillary-wave regime to criticality can come only from a theory which does not neglect "compressibility," i.e., density-density fluctuations in the bulk. For a discussion of the present status of the theory the series of papers by Sengers and van Leeuwen may be consulted.[3]

Some understanding may be gained by studying simple models yielding exact results, and in the present paper we study the interface in a particular version of the $d=2$ Ising model. Our system is an Ising $M \times \infty$ strip described fully in Sec. IV and depicted in Fig. 1, for which we calculate the correlation length ξ along the interface. Comparison with the known results for the solid-on-solid (SOS) model (recalled in Sec. III) is interesting and is given in Sec. IV.

II. THE DENSITY-DENSITY CORRELATION FUNCTION

For a two-dimensional strip infinite in one direction the lattice model can be treated and often solved with the aid of the transfer matrix.[4] The density-density correlation function

$$H(1,2) \equiv \langle \rho(1)\rho(2) \rangle - \langle \rho(1) \rangle \langle \rho(2) \rangle \tag{2.1}$$

can be expressed as

$$H(1,2) = H(z_1, z_2; \Delta x) = \Sigma_n A_n(z_1, z_2)(\lambda_n/\lambda_1)^{\Delta x} , \tag{2.2}$$

with $n > 1$, $\Delta x \neq 0$ where the index n labels the eigenvalues of the transfer matrix $\lambda_1 > \lambda_2 > \cdots$. If we keep M finite λ_2/λ_1 dominates at large $\Delta x \gg M^r$ and then quite generally we may identify

$$\lambda_2/\lambda_1 = \exp(-1/\xi_\perp) . \tag{2.3}$$

An anisotropic object such as a planar interface ought to produce two correlation lengths $\xi_\perp$ and $\xi_\parallel$ controlling the decay of H in the x and z directions, respectively. In addition to these two lengths, there is the ubiquitous bulk correlation length ξ_b. The density profile $\bar{\rho}(z)$, or the magnetization profile $m(z) = 2\bar{\rho}(z) - 1$, has its own length scale W, the width of the interface. If the interface is held in place by an external gravitational potential, the scaling relation predicted by capillary-wave theory[2] is

$$\xi_\perp = 2\beta\Gamma W^2 , \tag{2.4}$$

in which the external potential does not appear explicitly. Here $\beta = 1/kT$ is the inverse temperature and Γ is the stiffness of the interface. We remark that if we were to study the adsorption at the wall it would be customary to denote $\xi_\perp$ as "parallel" to the wall, but here we keep to the well-established terminology used for floating interfaces which become planar *only* under the influence of an

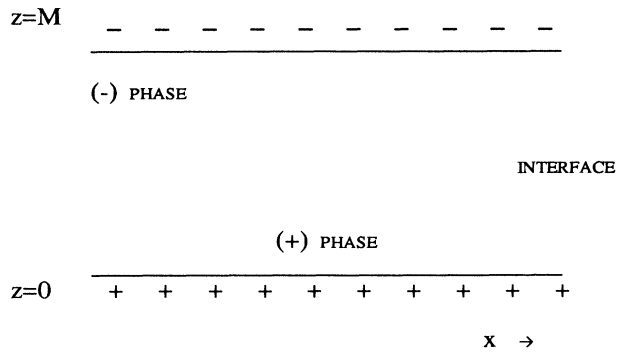

FIG. 1. The $M \times \infty$ strip with $(+/-)$ boundary conditions, i.e., with two rows of fixed spins at $z=0$ and M with $(+)$ spins below and $(-)$ spins above. The x direction is along the walls.

external field $V(z)$ and so $\xi_\perp$ "along" the planar interface is then *transverse* with respect to the field.

It is important to remark that the ratio (2.3) gives the *ultimate* rate of decay of $H(\ldots,\Delta x)$, i.e., after all terms related to higher eigenvalues in the sum (2.2) have died out and (2.3) dominates. As M increases, the eigenvalues are separated by smaller and smaller gaps and therefore condition on $\Delta x \gg M^r$ is more and more stringent; e.g., for the SOS model the exponent r given above is[5] $r=2$. The function H as defined in (2.1) is equal to $\frac{1}{4}$ of the spin-spin correlation function discussed in Sec. IV.

III. THE SOS STRIP

The correlation length for the x direction (parallel to the interface) can be extracted from the exact results obtained for the SOS semi-infinite strip.[5] Consider an $M\times\infty$ strip, such as that depicted in Fig. 1, of the plane square lattice with an Ising spin $\sigma=\pm1$ on each lattice site. In the SOS model the dense phase contains $\sigma=+1$ (plus) spins only and the other, $\sigma=-1$ (minus) spins only; overhangs of the dividing line between the two phases are excluded. It follows that the microscopic configuration is given by a collection of heights $\{h_i\}$, where i numbers the columns and in our case $0\le h_i\le M$ for each i. The column-column transfer matrix in the x direction,

$$T_{hh'}=\exp[-2K|h-h'|]\ , \tag{3.1}$$

has been diagonalized[5] and its eigenvalues are

$$\lambda_n=\frac{\sinh 2K}{\cosh 2K-\cos(n\pi/M)}\ . \tag{3.2}$$

The interface stiffness is $\beta\Gamma=2\sinh^2 K=\cosh 2K-1$. Using now the relation (2.3) we obtain

$$-1/\xi_{\rm SOS}=\ln\frac{\beta\Gamma+1-\cos(\pi/M)}{\beta\Gamma+1-\cos(2\pi/M)}\ . \tag{3.3}$$

Expanding in powers of $1/M$ while keeping $\beta\Gamma$ constant we obtain

$$1/\xi_{\rm SOS}=(3\pi^2/2\beta\Gamma)M^{-2}+\cdots,\quad \beta\Gamma\neq0, M^{-1}\to0\ . \tag{3.4}$$

Since the width of the interface was found to be[5] $W=\pi/M$, we obtain agreement with the scaling relation (2.4) of capillary-wave theory. Even though the interface is localized only by the finite size of the strip in the z direction, the form of (2.4) is preserved. The numerical coefficient is altered [note the factor of 3 in (3.4)]. We still have $\xi_\perp\sim\Gamma$ and $\xi_\perp\sim W^2$. The SOS model has no critical point and $\beta\Gamma$, $\xi_\perp$, and all other quantities vary monotonically with K. At the critical point of the isotropic [$K\equiv K_1=K_2$ in (4.1) below] Ising model with the same value of K, $\beta\Gamma=\sqrt{2}-1$ and $\xi_\perp$ takes the value given by (3.3) exactly or by (3.4) approximately.

IV. THE ISING INTERFACE IN THE (+/−) STRIP

Consider an Ising strip periodic in the x direction $x\in[1,L]$, $L\to\infty$, $z\in[0,M]$, with two boundaries $\sigma(x,0)=+1$ and $\sigma(x,M)=-1$, as depicted in Fig. 1. The Hamiltonian is

$$\beta\mathcal{H}=K_1\Sigma\Sigma\sigma(x,z)\sigma(x+1,z)+K_2\Sigma\Sigma\sigma(x,z)\sigma(x,z+1)$$
$$+K_2\Sigma\Sigma\sigma(x,0)\sigma(x,1),\quad \sigma(\ ,\ )=\pm1 \tag{4.1}$$

$$\beta=1/kT,\quad z=1,\ldots,M-1,\quad x=1,\ldots,L$$
$$\text{(cyclical, } L\to\infty)\ . \tag{4.2}$$

The column-column transfer matrix in the x direction is easily constructed; it has been diagonalized by Abraham and Martin-Löf;[6] Ref. 6 treats the case we need in which all $\sigma(x,z=0)$ are equal, as are all $\sigma(x,z=M)$. The solution in Ref. 6 contains all four cases: $+|\cdots|+$, $-|\cdots|-$, $-|\cdots|+$, and $+|\cdots|-$. We extract the last case for which $\sigma(x,0)=+1$ and $\sigma(x,M)=-1$. In the general solution the eigenvalues are

$$\lambda_n=\exp[\tfrac{1}{2}(\pm\gamma_1\pm\gamma_2\pm\gamma_3\pm\cdots)]$$
$$=\Lambda_0\exp(-\gamma_{l_1}-\gamma_{l_2}-\cdots) \tag{4.3}$$

(each is doubly degenerate) and the set $|L\rangle=|l_1,l_2,l_3,\ldots\rangle$ specifies which γ's enter with a minus sign. The $+|\cdots|-$ case corresponds to an *odd* number of such $\exp(-\gamma_k)$ factors multiplying Λ_0. Since $\gamma_1<\gamma_2<\gamma_3<\cdots$ the largest eigenvalue is $\lambda_1=\Lambda_0\exp(-\gamma_1)$ and the next is $\lambda_2=\Lambda_0\exp(-\gamma_2)$ at all temperatures $T<T_c$. Hence the ratio of the eigenvalues is

$$\lambda_1/\lambda_1=e^{-G},\quad G=\gamma_2-\gamma_1=1/\xi_\perp\quad(G\equiv G_{+-})\ . \tag{4.4}$$

As explained in Sec. II, this ratio controls the *ultimate* decay (in the x direction) of the two-point spin-spin or density-density correlation function.

Expressions for γ_k are known from Ref. 6, e.g.,

$$\cosh\gamma_k=\cosh(v_2-v_1)$$
$$+\sinh(v_2)\sinh(v_1)(1-\cos\omega_k)\ , \tag{4.5}$$

$$v_2=2K_2,\quad v_1=2K_1^*,\quad \sinh 2K_1\sinh 2K_1^*=1\ , \tag{4.6}$$

and ω is a solution of

$$\delta'(\omega)=M\omega-(k-1)\pi,\quad \sin\delta'\sinh\gamma=\sin\omega\sinh v_2$$
$$(k=1,2,\ldots)\ , \tag{4.7}$$
$$\cos\delta'\sinh\gamma=\cosh v_2\sinh v_1-\sinh v_2\cosh v_1\cos\omega\ .$$

We performed detailed calculations for the case $K\equiv K_1=K_2$. The surface tension (free energy per unit length) is $v_0=\beta\sigma=v_2-v_1$ whereas the interface stiffness $\beta\Gamma=\sinh(v_0)$.[3-5] The quantity v_0 is directly related to the (isotropic) bulk correlation length in the infinite system; above T_c, $1/\xi_b=|v_0|$ and below T_c, $1/\xi_b=2v_0$. We use these quantities below.

Equations (4.7) reduce to a transcendental equation for ω which is to be solved for each k with the condition $M\omega_k\in[(k-1)\pi,k\pi]$. We solve it for two roots ω_1 and ω_2 with $0<\omega_1<\pi/M<\omega_2<2\pi/M$. The equation can be written as[7]

$$\tan(M\omega)=\sin\omega/(a-b\cos\omega)\ ,$$
$$a\equiv b/\sinh v_2,\quad b\equiv\coth(v_1)\ . \tag{4.8}$$

The right-hand side (rhs) of (4.8) does not depend on M; at each temperature it is a smooth function of ω. A detailed discussion of the behavior of the solutions allows us to distinguish different regions of temperature for fixed M. At low temperatures the rhs of (4.8) is negative and decreasing for small ω and solutions for ω_1 and ω_2 are found for $\pi/2M<\omega_1<\pi/M$ and $3\pi/2M<\omega_2<\pi/M$, i.e., where the lhs is also negative. Anticipating the results to be described below we call this region the scaling region. As T_c is approached from below, the zero of the denominator $\omega^*(T)$ approaches $\omega^*=0$ and eventually ω_2, and then ω_1, are found for the lhs and rhs positive. At T_c the equation takes the form

$$\tan(M\omega)=(1/\sqrt{2})\sin\omega/(1-\cos\omega)\ . \tag{4.9}$$

Now the rhs varies as $+\sqrt{2}/\omega$ for small ω, quite unlike in the scaling region. Above T_c there is a small region $T_c<T<T_{\max}(M)$ where ω_1 is still real and positive. $T_{\max}$ is given by[8]

$$\coth(v_1)[1/\sinh(v_2)-1]=1/M\ . \tag{4.10}$$

Above $T_{\max}$ we have a situation mentioned in Ref. 6, namely ω_1 turns out to be pure imaginary and is not determined from (4.7) and (4.8). An estimate of ω_1 has been given there.[6] Recently ω_1 and the corresponding eigenvector have been calculated.[8] Here we need only the condition (4.10), which is exact. As $(1/M)\to 0$, $T_{\max}\to T_c^+$ as $(1/M)^2$.

Thus we have a region of high temperature $T>T_{\max}(M)$ plus two other regions of temperature that are of interest to us: (i) near critical where the equation is solved by positive lhs and rhs of (4.8) and (ii) the remaining region, where (4.8) is solved at negative lhs and rhs. For region (ii) we derive below the scaling law for $\xi_\perp$. Note, however, that the solutions ω_1 and ω_2 vary continuously with T at constant M, in the entire interval $0<T<T_{\max}(M)$.

Having solved for $\omega_1(T,M)$ and $\omega_2(T,M)$ we substitute into (4.5) to find γ_1, γ_2, and $1/\xi_\perp$ from (4.4). Figure 2 shows a particular example with $M=91$; the exact $1/\xi_\perp$ for the Ising strip is compared with $1/\xi_{\rm SOS}$ for the SOS model given by (3.3). At low temperatures the agreement is excellent and $\xi_\perp$ is very large because of the long-range capillary-wave fluctuations. Near T_c, $\xi_\perp$ (Ising) begins to *decrease* and crosses over smoothly to become indistinguishable from bulk ξ_b just above $T_{\max}(M)$. The figure also shows $1/\xi_b$ above T_c, strictly speaking the infinite system value, $1/\xi_b^\infty$. We do not complicate the figure with data for other values of M; the larger M the sooner $\xi_\perp$ (Ising) deviates from $\xi_{\rm SOS}$. As the data end at $T_{\max}(M)$, the curve may not merge with $\xi_b(T)$ before $T_{\max}$, but the trend is apparent.

At T_c the solutions of (4.9) are found numerically as everywhere else and also by straightforward expansion in powers of $1/M$. We find

$$(\xi_\perp^c)^{-1}=G_c(M)\ ,\quad G_c(M)=G_1/M+G_2/M^2+\cdots\ , \tag{4.11}$$

with

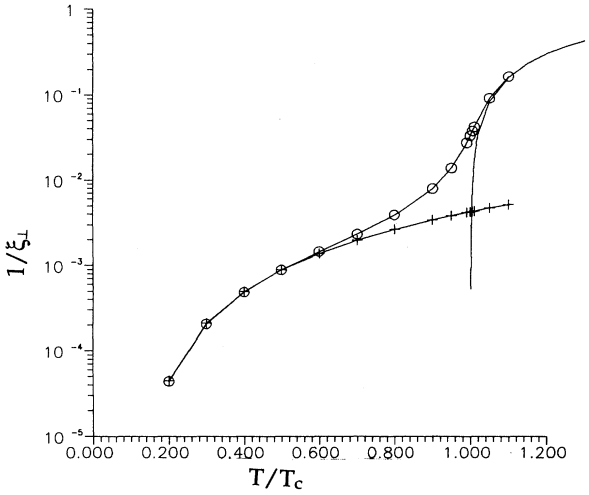

FIG. 2. $1/\xi_\perp$ is plotted vs T/T_c for the Ising $M\times\infty$ strip (circles) and the corresponding SOS strip (crosses). Here $M=91$. The line is $1/\xi_b^\infty$. Note that, far from T_c, $\xi_\perp$ already differs from $\xi_{\rm SOS}$ by several orders of magnitude.

$$G_1=\pi,\quad G_2=-\pi/\sqrt{2},\quad G_3=\pi[-\tfrac{13}{48}\pi^2+\tfrac{1}{2}]\ ,$$
$$G_4=\pi(13/12\pi^2-\tfrac{1}{2})\sqrt{2}\ , \tag{4.12}$$
$$G_5=\pi(121/1536\pi^4-65/48\pi^2+\tfrac{1}{4})\ .$$

These $(G_2,G_3,\ldots)$ represent corrections to scaling.

Fixing the temperature at any value below T_c and expanding in powers of $1/M$ implies M sufficiently large. Then solutions for ω occur for negative lhs=rhs of (4.8). We find

$$\gamma_k=(1/2\beta\Gamma)(k\pi)^2/M^2+O(M^{-3})\ , \tag{4.13}$$

as found earlier by Abraham and Svrakic.[9] Hence

$$1/\xi_\perp=G=(3\pi^2/2\beta\Gamma)M^{-2}+\cdots\ ,\quad M\to\infty\ . \tag{4.14}$$

As $1/M$ vanishes at constant T below the critical region, the exact $1/\xi_\perp$ (Ising) is reproduced (to the dominant power of $1/M$) by $1/\xi_{\rm SOS}$ of the SOS model, obtained from (3.4), for the same stiffness $\beta\Gamma$. Therefore we see that the result expressed in (4.14)—although rigorously correct for the Ising strip and obtained in a well-defined limit of $(1/M)\to 0$ at any constant temperature below the critical point $T<T_c$—pertains to the capillary-wave class of results.

We note that the interface stiffness $\beta\Gamma$ must be nonzero otherwise (4.14) and its derivations are not valid. At $T=T_c$ (4.14) is replaced by (4.11). At the next power of $1/M$ we obtain

$$1/\xi_{\rm SOS}=\tfrac{3}{2}(\pi/M)^2/\beta\Gamma$$
$$-\tfrac{5}{8}(\pi/M)^4[1/\beta\Gamma+3/(\beta\Gamma)^2]+\cdots \tag{4.15}$$

(with, strictly, $\beta\Gamma=2\sinh^2K$ for the SOS model) whereas

$$1/\xi_\perp(\text{Ising})=\tfrac{3}{2}(\pi/M)^2/\beta\Gamma + 3(\pi^2/M^3)/[\beta\Gamma(a-b)]+\cdots \quad (4.16)$$

with $\beta\Gamma=\sinh v_0$ and $a-b=-\beta\Gamma+\ldots$. to a first approximation.

In general $\xi_\perp(\text{Ising})=\xi_\perp(T,M)$ and it is compelling to consider two obvious dimensionless ratios $M/\xi_\perp$ and M/ξ_b (remembering that for $d=2$ Ising models $\nu=1$). For ξ_b we take the correlation length of the infinite homogeneous system $1/\xi_b^\infty=v_0=v_2-v_1$. Plotting $MG=M/\xi_\perp$ vs Mv_0 we obtain a very good common curve. In place of Mv_0 we can use equally well $M|T/T_c-1|$ or $M|T/T_{\max}(M)-1|$. Replacing v_0 by $\beta\Gamma=\sinh(v_0)$, the interface stiffness, i.e., using the variable $X=M\sinh v_0$, an excellent scaling plot is obtained, shown in Fig. 3. The scaling extends to very large values of $M\beta\Gamma$ and in this respect it is superior to the plot against Mv_0. The corrections to scaling given by (4.12) are barely visible on the scale of the graph.

The scaling function Y in

$$M/\xi_\perp=Y(M\sinh v_0) \quad (4.17)$$

can be found under the assumptions $1/M\to 0$, $\sinh v_0\to 0, M\sinh v_0\sim O(1)$. Then $\gamma_k\sim 1/M$ $(k=1,2)$, $\cosh\gamma_k=1+\gamma_k^2/2$, and expanding the rhs of (4.5) in powers of $\sinh v_0$, for $T<T_c$, we find

$$\gamma_k^2=[\sinh(v_0)]^2+\omega_k^2 , \quad (4.18)$$

or introducing the variable $X=M\sinh v_0$,

$$(M\gamma_k)^2=X^2+(M\omega_k)^2 . \quad (4.19)$$

Hence, if scaling is to be consistent, ω_k must be $O(1/M)$ and $O[\sinh(v_0)]$—at least for $k=1,2$. Then for small $1/M$, ω is small, and the rhs of (4.8) can be expanded

$$\tan(M\omega_k)=\frac{\omega_k-\omega_k^3/3!}{-\sinh(v_0)+\omega_k^2/\sqrt{2}} =\frac{M\omega_k+\cdots}{-X+\cdots} \quad (k=1,2) \quad (4.20)$$

or

$$-X=Z_k\cot(Z_k) \quad (4.21)$$

with $Z_k\equiv M\omega_k$. If $T<T_c$, $Z_k>0$, $X>0$, and $\cot Z_k<0$ for both $k=1,2$. Applying (4.19) twice we find

$$MG=M/\xi_\perp=Y(X)=(X^2+Z_1^2)^{1/2}-(X^2+Z_2^2)^{1/2} , \quad (4.22)$$

where Z_1Z_2 are solutions of (4.21)—one in the interval $0<Z_1<\pi$ (but in fact $\pi/2<Z_1<\pi$) and the other in the interval $\pi<Z_2<2\pi$ (but in fact $3\pi/2<Z_2<2\pi$). In this way (4.22) and these two conditions on the two roots of (4.21) fully determine the scaling function Y.

We can expand Y systematically about $X=0$ for which $Y(0)=\pi$ and alternatively about $1/X=0$ for which $Y(\infty)=0$. Solutions of (4.21) are expanded first. One obtains for small X

$$\begin{aligned}
&MG=A_0+A_1X+A_2X^2+\cdots ,\\
&A_0=\pi ,\\
&A_1=-\tfrac{4}{3}/\pi ,\\
&A_2=(-\tfrac{2}{3}\pi^2+\tfrac{208}{27})/\pi^3 ,\\
&A_3=(\tfrac{520}{81}\pi^2-\tfrac{15\,488}{243})/\pi^5 ,\\
&A_4=(\tfrac{26}{27}\pi^4-\tfrac{54\,208}{729}\pi^2+\tfrac{1\,399\,040}{2187})/\pi^7 ,\\
&A_5=(-\tfrac{86\,152}{3645}\pi^4+\tfrac{699\,520}{729}\pi^2-\tfrac{141\,080\,576}{19\,683})/\pi^9 ,\\
&A_6=(-\tfrac{484}{243}\pi^6+\tfrac{15\,354\,464}{328\,05}\pi^4-\tfrac{775\,943\,168}{590\,49}\pi^2+\tfrac{5\,079\,130\,112}{590\,49})/\pi^{11} ,\\
&A_7=(\cdots) .
\end{aligned} \quad (4.23)$$

Here $X<\pi$. Alternatively, for large X,

$$\begin{aligned}
&M/\xi_\perp=MG=B_1X^{-1}+B_2X^{-2}+\cdots ,\\
&B_1=\tfrac{3}{2}\pi^2 ,\\
&B_2=-3\pi^2 ,\\
&B_3=\pi^2(-\tfrac{15}{8}\pi^2+\tfrac{9}{2}) ,\\
&B_4=\pi^2(\tfrac{25}{2}\pi^2-6)\\
&B_5=\pi^2(\tfrac{63}{16}\pi^4-\tfrac{175}{4}\pi^2+\tfrac{15}{2}) ,\\
&B_6=\pi^2(-\tfrac{1869}{40}\pi^4+\tfrac{225}{2}\pi^2-9) .
\end{aligned} \quad (4.24)$$

Here $X^{-1}<\frac{1}{2}\pi$. A_0 agrees with G_1 from (4.12).

It is quite satisfactory that the expansion (4.24) and, therefore, the scaling function Y contain the earlier result (4.14) [and 4.13 (Ref. 9)] as a limiting case. Keeping only

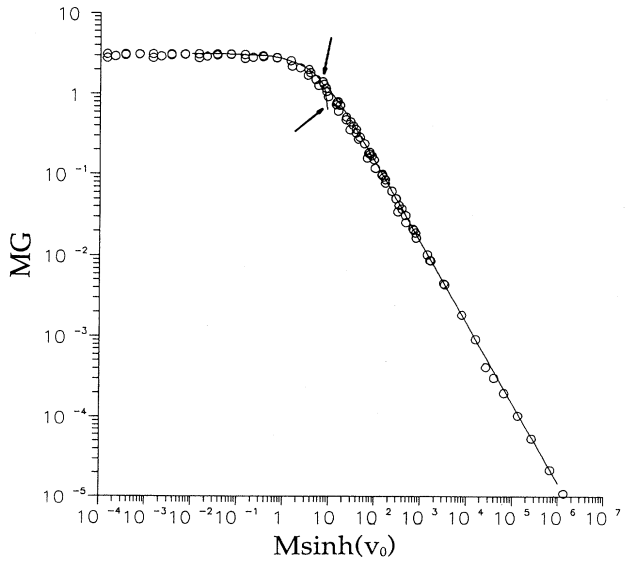

FIG. 3. The scaling plot for the $+/-$ gap $G=1/\xi_\perp$, $M=8$–400, $T/T_c\in[0.1,1]$ in variables $M/\xi_\perp\equiv MG$ and $X=M\sinh v_0$ with the region $10^{-8}<X'<10^{-4}$ (where MG is practically constant) omitted for clarity. The lines represent expansions of the scaling function, Eqs. (4.23) and (4.24).

the first term in the expansion for *large* scaling variable X, we obtain

$$M/\xi_\perp = B_1 X^{-1} \quad \text{or} \quad 1/\xi_\perp = B_1 M^{-2}/\sinh(v_0) , \quad (4.25)$$

thereby recovering (4.14) in view of the (exact) value of B_1. Thus the earlier Ising result and the corresponding SOS result (including the M^{-2} size dependence) are now understood; (4.14) is the large X limit of the scaling function (4.22), i.e., exactly the first term of the expansion (4.24). Large X means large M and/or low temperature.

The expansions (4.24) and (4.25), truncated after the first six terms, reproduce the exact data (plotted in Fig. 3) very satisfactorily; the two arrows point to their respective breakdown. The numerical calculation of the scaling function (4.21) and (4.22) is indistinguishable on the scale of the graph from these expansions in the respective regions of their validity.

V. DISCUSSION

For low dimensionality $d < 3$, obtaining a fundamental description of the vanishing of the interfacial density (magnetization) profile as the critical temperature is reached is an interesting problem in statistical mechanics. Some partial understanding can be reached by studying simple models such as the $(+/-)$ Ising strip considered in this paper. Before the full spin-spin correlation function is studied, we have investigated its long-distance correlation length $\xi_\perp$ in the direction along the interface. We find a physically attractive picture of a crossover from low temperatures, where the correlation length is practically the same as for the solid-on-solid strip with the same width and the same coupling constant, through a region near the critical temperature where $\xi_\perp$ is progressively smaller than the SOS value, to temperatures *above* T_c where $\xi_\perp$ crosses over to (small) values practically equal to the bulk correlation length of an infinite Ising system.

The physical significance of this behavior is appreciated if one realizes that the SOS model is nothing more than a realization of the capillary-wave model on a lattice. At low temperatures therefore the exact $\xi_\perp$ shows all the properties (attributes) of the capillary length.

It is perhaps relevant that the bulk correlation length $\xi_b(T)$ *above* T_c enters into the picture whereas the other branch, omitted from Fig. 2 for clarity, of $\xi_b(T)$ *below* T_c seems to be entirely unrelated. The only observation one might make is that, when raising T, $\xi_\perp(T)$ begins to fall rapidly about when $\xi_\perp \sim \xi_b \sim M$ or earlier. As we pointed out in Sec. IV, the exact result expressed in (4.14) pertains to the capillary-wave class of results and $\xi_b(T)$ does not enter there.

We have also determined the scaling relation for $\xi_\perp$, covering an extremely wide range of the scaling variable, which is the interface stiffness multiplied by the strip width. The scaling equation is valid near T_c and also in the low-temperature regime where it embraces the dominant M^{-2} behavior of large strips found both for Ising and SOS models. Thus there is no correction at low temperatures which the bulk density fluctuations would introduce into the simple capillary-wave $\xi_\perp$. The last statement, however, must be qualified by the remark that this is true to dominant order of $1/M$. The other qualification concerns the particular scale of distances to which our calculation applies. As mentioned in Sec. II the correlation function decay is ruled by λ_2/λ_1 *only* (with neglect of higher eigenvalues) at asymptotically large distances $\Delta x \gg M^r$ where r has been determined[5] for the SOS model as $r=2$. A study of distances $\Delta x \sim M$ for the strip considered here is currently under way.

ACKNOWLEDGMENTS

The author is greatly indebted to Dr. A. Ciach, A. Maciolek, and A. Poniewierski for several discussions. He is also grateful to Dr. J. M. J. van Leeuwen for a very illuminating discussion and to Professor R. Evans for a critical reading of the manuscript.

APPENDIX

Once the quantities γ_1 and γ_2 for given M and T are computed one can immediately find the correlation length parallel to the long edge of an $M \times \infty$ strip with the $(+/+)$ boundary condition. In the general solution (4.3) the $+|\cdots|+$ case corresponds to an *even* number of $\exp(-\gamma_k)$ factors multiplying Λ_0. Now the largest eigenvalue is $\lambda_1 = \Lambda_0$ and the next is $\lambda_2 = \Lambda_0 \exp(-\gamma_2 - \gamma_1)$ at all temperatures $T < T_c$. Hence the ratio of the eigenvalues is

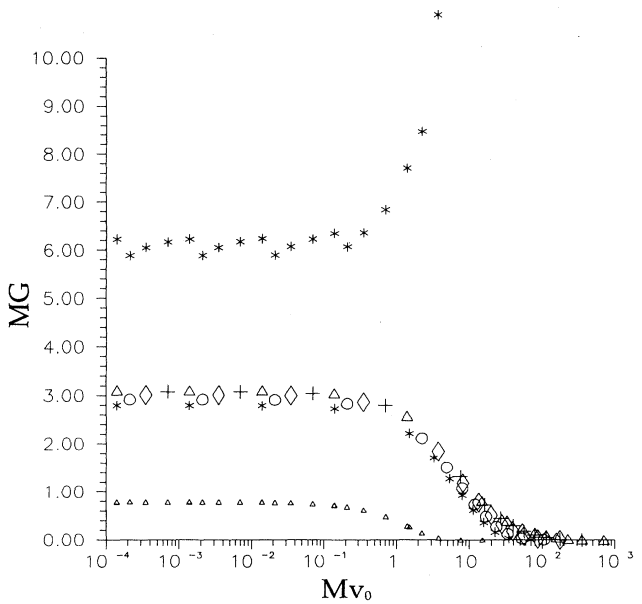

FIG. 4. Gap $G_{++} = 1/\xi_{++}$ (stars) for $(+/+)$ boundary condition compared with G_{per} (triangles) for periodic boundary conditions and with gap $G_{+-} = 1/\xi_\perp$, computed numerically for $M=8$ (stars), $M=12$ (circles), $M=20$ (diamonds), $M=40$ (crosses), and $M=80$ (large triangles), for $T/T_c \in [0.8,1]$ for $(+/-)$ fixed-spin boundaries, all plotted against $Mv_0 = M/2\xi_b^\infty$. The scaling region near $Mv_0 \sim 1$, the corrections to scaling as $Mv_0 \to 0$ where each system reaches its own critical gap, and the low-temperature region where $X = M \sinh v_0$ is a better variable than Mv_0 are all visible.

$$\lambda_2/\lambda_1 = e^{-G_{++}}, \quad G_{++} = \gamma_2 + \gamma_1 = 1/\xi_{++} . \tag{A1}$$

Figure 4 shows a plot of $MG_{++} \equiv M/\xi(++)$ vs Mv_0. For the sake of comparison the case of periodic boundary conditions and the $(+/-)$ case are also included. MG_{++} starts from a value near 2π for $T \approx T_c$ and increases immediately to values corresponding to a microscopic correlation length appropriate for a pure $(+)$ phase. We can also see the corrections to scaling very close to T_c. G_{++} at T_c can be readily found using the analytical solution(s) of (4.9) which we already obtained by systematic expansion in $1/M$. Hence

$$1/\xi(++, T_c, M) = G^c_{++} = g_1/M + g_2/M^2 + \cdots , \qquad g_1 = 2\pi, \quad g_2 = -\pi\sqrt{2}, \quad g_3 = \pi(-\tfrac{7}{24})\pi^2 + 1) \cdots . \tag{A2}$$

These $(g_2, g_3 \ldots)$ represent corrections to scaling, since Fig. 4 suggests ξ_{++} should also scale as $M/\xi_{++} = F(M/\xi_b)$.

For a strip with periodic boundary conditions in zero field the gap is given by[10]

$$G_{\text{per}} = 1/\xi_\perp = \Sigma_k [\gamma(2k + 1/m) - \gamma(2k/m)], \qquad k = 0, \ldots, M-1 \tag{A3}$$

where $\gamma(\omega)$ is given again by a solution of (4.5). Here $m = M/\pi$ and there is no transcendental equation to solve for ω. We used (A3) for a numerical calculation of G_{per} plotted in Fig. 4. It illustrates the fact that the behavior of the $(+/-)$ strip cannot be deduced from (mostly known) results for other boundary conditions.[11] On the scale of Fig. 4 we can also see the corrections to scaling near and at T_c.

[1] F. P. Buff, R. A. Lovett, and F. H. Stillinger, Phys. Rev. Lett. **15**, 621 (1965); see also, e.g., J. S. Rowlinson and B. Widom, *Molecular Theory of Capillarity* (Oxford University Press, Oxford, 1982).

[2] M. Wertheim, J. Chem. Phys. **65**, 2377 (1976); J. D. Weeks, *ibid.* **67**, 3106 (1977); D. Bedeaux and J. D. Weeks, *ibid.* **82**, (1985); see also R. Evans, Course 1 in *Liquids at Interfaces,* 1988 Les Houches Session XL VIII (Elsevier, New York, 1990).

[3] See J. V. Sengers, J. M. J. van Leeuwen, and J. W. Schmidt, Physica A **172**, 20 (1991); J. M. J. van Leeuwen, J. Stat. Phys. **57**, 433 (1989); J. V. Sengers and J. M.J. van Leeuwen, Phys. Rev. A **39**, 6346 (1989); J. M. J. van Leeuwen and J. V. Sengers, Physica A **137**, 156 (1986); **137**, 178 (1986), where references to earlier papers can be found.

[4] H. J. Hilhorst and J. M. J. van Leeuwen, Physica A **107**, 319 (1981); see also, e.g., D. B. Abraham, in *Phase Transitions and Critical Phenomena,* edited by C. Domb and J. L. Lebowitz (Academic, New York, 1986), Vol. 10.

[5] A. Ciach, Phys. Rev. B **34**, 1932 (1986); A. Ciach, J. Dudowicz, and J. Stecki, Phys. Rev. Lett. **56**, 1482 (1986); A. Ciach and J. Stecki, J. Phys. A **20**, 5619 (1987); P. C. Hemmer and B. Lund, *ibid.* **21**, 3463 (1988); P. C. Hemmer and J. Stecki, *ibid.* **23**, 1735 (1990). For a more general discussion of the SOS model(s), though mostly under different boundary conditions, see A. Kooiman, J. M.J. van Leeuwen, and R. K. P. Zia, Physica A **170**, 124 (1990); M. N. Svrakic, V. Privman, and D. B. Abraham, J. Stat. Phys. **53**, 1041 (1988).

[6] D. B. Abraham and A. Martin-Löf, Commun. Math. Phys. **32**, 245 (1973).

[7] K. Olaussen and K. H. Haugholt (unpublished); K. H. Haugholt, M.Sc. thesis, University of Trondheim, 1989.

[8] A. Maciolek and J. Stecki (unpublished).

[9] D. B. Abraham and N. M. Svrakic, Phys. Rev. Lett. **56**, 1172 (1986).

[10] V. Privman and M. E. Fisher, J. Stat. Phys. **33**, 385 (1984), Appendix B.

[11] T. W. Burkhardt and I. Guim, Phys. Rev. B **35**, 1799 (1987).